Robotica (2012) volume 30, pp. 343–349. © Cambridge University Press 2011
doi:10.1017/S0263574711000622

Dimensional synthesis of the Delta robot using transmission angle constraintsDimensional synthesis of the Delta robot using transmission angle constraints

LiMin Zhang, JiangPing Mei*, XueMan Zhao and Tian Huang

School of Mechanical Engineering, Tianjin University, Tianjin 300072, China

(Received in Final Form: May 26, 2011; accepted May 24, 2011. First published online: July 1, 2011)

SUMMARY

This paper deals with dynamic dimensional synthesis of the Delta robot using the pressure/transmission angle constraints. Two types of pressure/transmission angles are defined, with which the direct and indirect singularities can be identified in a straightforward manner. Two novel global dynamic metrics are proposed for minimisation, which are associated respectively with the inertial and centrifuge/Coriolis components of the driving torque. Various geometrical and performance constraints are taken into account in terms of workspace/machine volume ratio, pressure/transmission angles, etc. The effects of pressure/transmission angle constraints on the feasible domain of design variables are investigated in depth via an example, and a set of optimised dimensional parameters is obtained for achieving a good kinematic and dynamic performance throughout the entire task workspace.

KEYWORDS: Parallel robot; Transmission angle; Dimensional synthesis; Design; Dynamic performance.

1. Introduction

In recent years, the parallel manipulators actuated by the proximal revolute joints have widely been employed to conduct high-speed pick-and-place operations in electronics, packaging, pharmacy and many other light industries. This statement can be exemplified by the very successful applications of the 2-DOF Diamond robot,[1,2] 3-DOF Delta robot,[3,4] as well as 4-DOF H4[5] and Par4[6] robots with two to three pure translational and/or three translational plus one rotational movement capabilities.

Dimensional synthesis is an important design issue in the development of such robots, which is primarily concerned with the determination of a set of geometric parameters by optimising a cost function subject to a set of appropriate constraints. The approaches in previous work dealing with this problem may be classified into two categories, i.e. kinematic and dynamic dimensional synthesis, depending upon the cost function to be optimised.

The kinematic dimensional synthesis of parallel robots has been extensively investigated. The common routine is to optimise a conditioning index generated by algebraic characteristics of the Jacobian matrix, the condition number, determinant and minimum singular value, etc. The earlier work in this phase mainly focused upon finding the parametric loci necessary to generate an isotropic configuration.[7–11] Considering the global kinematic performance not being guaranteed by merely conducting local optimum design, Gosselin and Angeles[12] proposed a global conditioning index represented by the mean value of reciprocal of conditioning number of the Jacobian for maximisation. This index together with many modified versions has been widely employed for the kinematic design of the parallel manipulators actuated by the proximal revolute joints. For example, Miller[13,14] proposed a weighted cost function for maximisation, where the weights were associated, respectively, with mean value of the condition number and the volumetric ratio of the task workspace to the reachable workspace. Nabat *et al.*[6] investigated the dimensional synthesis problem of a Par4 robot by maximising the ratio of task workspace/machine volume provided that the workspace was bounded by a prescribed condition number. Laribi *et al.*[15] introduced the concept of power of a point to evaluate kinematic performance of the Delta robot within a prescribed workspace. Chio *et al.*[16] evaluated the kinematic performance of a H4 robot using the manipulability ellipsoid. By taking a 2-DOF translational parallel robot as an example, Huang *et al.*[17] found that condition number of the Jacobian was unable to describe the degeneration of the direct Jacobian when the platform moves along the symmetrical axis of a rectangular task workspace. Therefore, the minimum acute angle between the proximal and distal links (i.e. transmission angle) had to be considered as an additional constraint. Although this consideration has been widely used to ensure the force transmission behaviour of the planar linkages,[18–20] little extension has been made to the design of spatial parallel manipulators probably due to the geometric complexity.

As to the high-speed parallel robots for pick-and-place operations, the inertia of movable components should be taken into account in the dimensional synthesis. Conventionally, this leads to minimising a dynamic metric generated by the algebraic characteristics of the inertia matrix. The metrics available at hand include the dynamic isotropy,[21] dynamic manipulability[22] and its modified version.[23] For the parallel manipulators actuated by proximal revolute joints, however, selecting a more instructive and

* Corresponding author. E-mail: ppm@tju.edu.cn

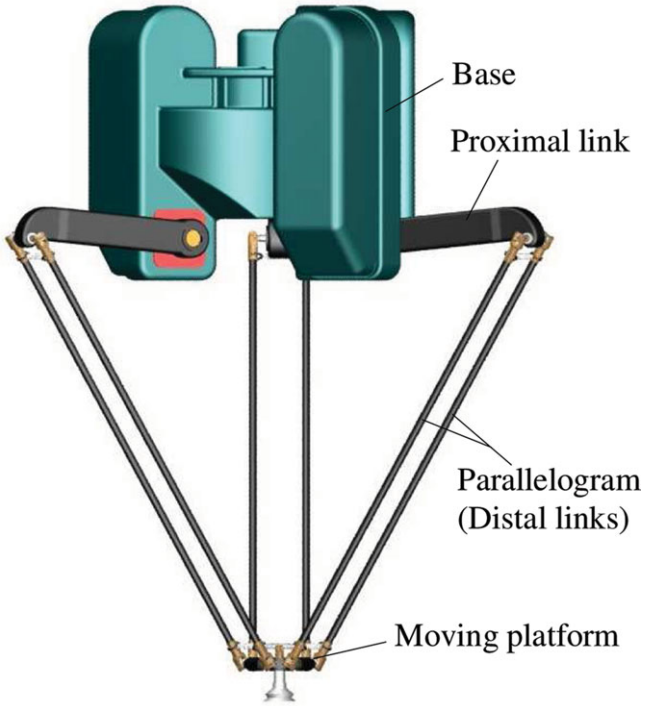

Fig. 1. (Colour online) 3D model of a Delta robot.

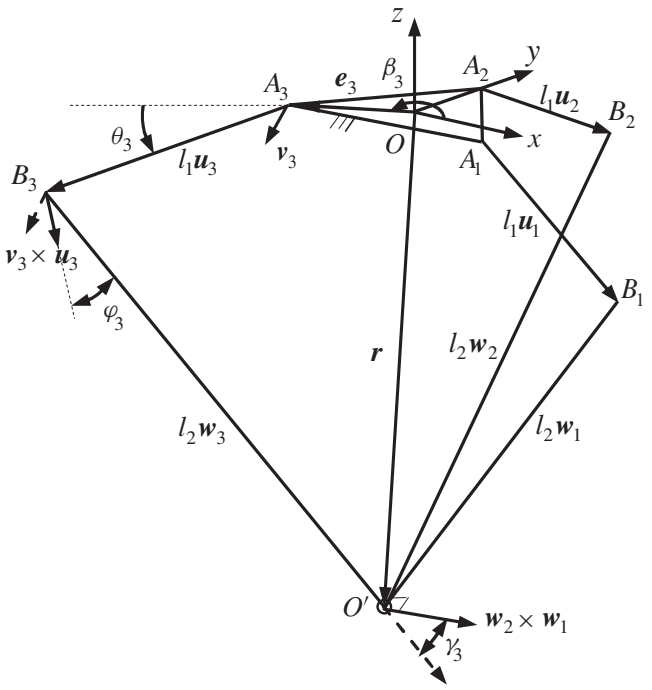

Fig. 2. Schematic diagram of the Delta robot.

meaningful dynamic metric remains an open problem to be tackled though many simplified dynamic models have been available at hand.[24–27]

By taking the Delta robot as an example, this paper deals with dynamic dimensional synthesis of high-speed parallel robot actuated by proximal revolute joints using transmission angle constraints. The paper is organised as follows. In Section 2, the inverse kinematic and rigid body dynamic analyses of the Delta robot are carried out. This is followed in Section 3 by the definition of two types of transmission angles. In Section 4, two novel global dynamic metrics are proposed for minimisation subject to a set of appropriate constraints in terms of the workspace/machine volume ratio and the transmission angles, etc. An example is given in Section 5 and the conclusions are drawn in Section 6.

2. Inverse Kinematics and Dynamics

In order to implement the dynamic dimensional synthesis, the inverse kinematic and dynamic analyses of the Delta robot are carried out as follows.

Figure 1 shows a 3D solid model of the Delta robot, which is composed of a base, a movable platform and three identical kinematic chains (limbs). The moving platform and active proximal link are made of aluminium alloy and the distal links are made of carbon fibre for a light-weight design.

Since the moving platform undergoes pure translation motion and the motions of two distal links within a parallelogram are identical, the kinematic model of the robot can be simplified as shown in Fig. 2. In the reference frame $O-xyz$, the position vector of point O' on the platform can be written as

$$r = e_i + l_1 u_i + l_2 w_i, \quad i = 1, 2, 3, \tag{1}$$

where $e_i = e(\cos\beta_i \ \sin\beta_i \ 0)^{\mathrm{T}}$ is the vector pointing from O to A_i (see Fig. 2), $\beta_i = (i-1)\frac{2\pi}{3} - \frac{\pi}{6}$; l_1,l_2, $\boldsymbol{u}_i$ and $\boldsymbol{w}_i$ are the lengths and unit vectors of the proximal and distal links, and

$$\boldsymbol{u}_i = (\cos\beta_i \cos\theta_i \sin\beta_i \cos\theta_i - \sin\theta_i)^{\mathrm{T}}, \tag{2}$$

where θ_i(i = 1,2,3) is the position angle of the ith proximal link.

The inverse position analysis gives

$$\theta_i = 2\arctan\frac{-E_i - \sqrt{E_i^2 - G_i^2 + F_i^2}}{G_i - F_i}, \quad i = 1, 2, 3, \tag{3}$$

where

$$E_i = 2l_1(\boldsymbol{r} - \boldsymbol{e}_i)^{\mathrm{T}}\hat{\boldsymbol{z}},$$
$$F_i = -2l_1(\boldsymbol{r} - \boldsymbol{e}_i)^{\mathrm{T}}(\cos\beta_i\hat{\boldsymbol{x}} + \sin\beta_i\hat{\boldsymbol{y}}),$$
$$G_i = (\boldsymbol{r} - \boldsymbol{e}_i)^{\mathrm{T}}(\boldsymbol{r} - \boldsymbol{e}_i) + l_1^2 - l_2^2.$$

$\hat{\boldsymbol{x}}$, $\hat{\boldsymbol{y}}$ and $\hat{\boldsymbol{z}}$ are the unit vectors of three orthogonal axes of the $O-xyz$. Thus, $\boldsymbol{u}_i$ can be determined by Eq. (2) and $\boldsymbol{w}_i$ can be determined by

$$\boldsymbol{w}_i = \frac{1}{l_2}(\boldsymbol{r} - \boldsymbol{e}_i - l_1\boldsymbol{u}_i). \tag{4}$$

Differentiating Eq. (1) with respect to time yields

$$\dot{\boldsymbol{r}} = l_1\dot{\theta}_i(\boldsymbol{v}_i \times \boldsymbol{u}_i) + l_2\boldsymbol{\omega}_i \times \boldsymbol{w}_i, \quad i = 1, 2, 3, \tag{5}$$

where $\dot{\boldsymbol{r}}$ is the velocity of O'; $\dot{\theta}_i$ is the magnitude of angular velocity of proximal link i; $\boldsymbol{\omega}_i$ is the angular velocity of the $i$thdistal link; $\boldsymbol{v}_i = (-\sin\beta_i \ \cos\beta_i \ 0)^{\mathrm{T}}$ is unit vector of the

https://doi.org/10.1017/S0263574711000622 Published online by Cambridge University Press

rotational axis of the ith proximal link, which is normal to the plane spanned by $\boldsymbol{e}_i$ and $\boldsymbol{u}_i$.

Taking the dot product with $\boldsymbol{w}_i$ on both sides of Eq. (5) and rewriting in matrix form gives the inverse velocity model of the robot

$$\dot{\boldsymbol{\theta}} = \boldsymbol{J}\dot{\boldsymbol{r}}, \tag{6}$$

where $\dot{\boldsymbol{\theta}} = (\dot{\theta}_1\ \dot{\theta}_2\ \dot{\theta}_3)^{\mathrm{T}}$; $\boldsymbol{J} = \boldsymbol{J}_q^{-1}\boldsymbol{J}_x$ is the Jacobian, and $\boldsymbol{J}_q = \mathrm{diag}[l_1\boldsymbol{w}_i^{\mathrm{T}}(\boldsymbol{v}_i \times \boldsymbol{u}_i)], \boldsymbol{J}_x = [\,\boldsymbol{w}_1\ \boldsymbol{w}_2\ \boldsymbol{w}_3\,]^{\mathrm{T}}$ are the direct and indirect Jacobian, respectively.

Again, differentiating Eq. (6) with respect to time leads to the inverse acceleration model of the system

$$\ddot{\boldsymbol{\theta}} = \boldsymbol{J}\ddot{\boldsymbol{r}} + \boldsymbol{f}(\dot{\boldsymbol{r}}), \tag{7}$$

where $\ddot{\boldsymbol{r}}$ is the acceleration of O'; $\ddot{\boldsymbol{\theta}} = \left(\ddot{\theta}_1\ \ddot{\theta}_2\ \ddot{\theta}_3\right)^{\mathrm{T}}$ with $\ddot{\theta}_i$ being the signed magnitude of the angular acceleration of the ith proximal link; and

$$\boldsymbol{f}(\dot{\boldsymbol{r}}) = (\,f_1(\dot{\boldsymbol{r}})\ f_2(\dot{\boldsymbol{r}})\ f_3(\dot{\boldsymbol{r}})\,)^{\mathrm{T}}, \tag{8}$$

where

$$f_i(\dot{\boldsymbol{r}}) = \dot{\boldsymbol{r}}^{\mathrm{T}}\boldsymbol{H}_i\dot{\boldsymbol{r}},$$

$$\boldsymbol{H}_i = \frac{1}{l_1^2\Delta_i}\left[\frac{(\boldsymbol{v}_i \times \boldsymbol{u}_i)^{\mathrm{T}}(\boldsymbol{v}_i \times \boldsymbol{w}_i)\,\boldsymbol{w}_i\boldsymbol{w}_i^{\mathrm{T}}}{\Delta_i^2} + \frac{l_1}{l_2}\left(\boldsymbol{E}_3 - \frac{(\boldsymbol{v}_i \times \boldsymbol{u}_i)\boldsymbol{w}_i^{\mathrm{T}}}{\Delta_i}\right)^{\mathrm{T}}\left(\boldsymbol{E}_3 - \frac{(\boldsymbol{v}_i \times \boldsymbol{u}_i)\boldsymbol{w}_i^{\mathrm{T}}}{\Delta_i}\right)\right],$$

$\Delta_i = \boldsymbol{w}_i^{\mathrm{T}}(\boldsymbol{v}_i \times \boldsymbol{u}_i)$, $\boldsymbol{E}_3$ is a unit matrix of order 3.

In the formulation of inverse dynamics, the following assumptions are made:

(1) Neglect friction and elasticity in joints;
(2) Referring to ref. [24], neglect moments of inertia of the distal links using the concept of static equivalent principle by which the mass of the link is divided and concentrated at the two endpoints B_i and O'.

Thus, the virtual work principle gives

$$(-m\ddot{\boldsymbol{r}} - mg\hat{\boldsymbol{z}})^{\mathrm{T}}\delta\boldsymbol{r} + (\boldsymbol{\tau} - I_{\mathrm{A}}\ddot{\boldsymbol{\theta}} - \boldsymbol{\tau}_{\mathrm{Ag}})^{\mathrm{T}}\delta\boldsymbol{\theta} = 0, \tag{9}$$

where $\boldsymbol{\tau} = (\,\tau_1\ \tau_2\ \tau_3\,)^{\mathrm{T}}$ is the actuated joint torque vector; m is the equivalent mass of the movable platform; I_{A} is the equivalent moment of inertia of the proximal link about the axis of rotation, including the contributions from motor rotor, active proximal link and the lumped mass of the distal links; $\boldsymbol{\tau}_{\mathrm{Ag}} = m_{\mathrm{A}}r_{\mathrm{A}}g(\cos\theta_1\ \cos\theta_2\ \cos\theta_3\,)^{\mathrm{T}}$ with $m_{\mathrm{A}}r_{\mathrm{A}}$ being the mass-radius product of the proximal link about its axis of rotation.

Substituting $\delta\boldsymbol{\theta} = \boldsymbol{J}\delta\boldsymbol{r}$ into Eq. (8) yields a set of inverse dynamic equations as follows:

$$\boldsymbol{\tau} = \boldsymbol{\tau}_a + \boldsymbol{\tau}_v + \boldsymbol{\tau}_{\mathrm{g}}, \tag{10}$$

where $\boldsymbol{\tau}_a$, $\boldsymbol{\tau}_v$ and $\boldsymbol{\tau}_g$ are the inertial, centrifuge/Coriolis and gravitational components, respectively,

$$\boldsymbol{\tau}_a = I_{\mathrm{A}}\boldsymbol{G}\ddot{\boldsymbol{r}}, \quad \boldsymbol{\tau}_v = I_{\mathrm{A}}\boldsymbol{f}(\dot{\boldsymbol{r}}), \quad \boldsymbol{\tau}_{\mathrm{g}} = mg\boldsymbol{J}^{-\mathrm{T}}\hat{\boldsymbol{z}} + \boldsymbol{\tau}_{\mathrm{Ag}},$$
$$\boldsymbol{G} = [(\eta\boldsymbol{J}^{-\mathrm{T}} + \boldsymbol{J})], \quad \eta = \frac{m}{I_{\mathrm{A}}}.$$

3. Pressure/Transmission Angles

In order to formulate the performance constraints in a visible manner, we define the pressure/transmission angles of the systems. Rewrite Eq. (6) such that

$$\dot{\boldsymbol{r}} = \boldsymbol{J}^{-1}\dot{\boldsymbol{\theta}}, \tag{11}$$

where

$$\boldsymbol{J}^{-1} = \boldsymbol{J}_x^{-1}\boldsymbol{J}_q, \quad \boldsymbol{J}_x^{-1} = \frac{1}{\Delta}[\,\boldsymbol{w}_3 \times \boldsymbol{w}_2\ \ \boldsymbol{w}_1 \times \boldsymbol{w}_3\ \ \boldsymbol{w}_2 \times \boldsymbol{w}_1\,],$$
$$\Delta = \boldsymbol{w}_1^{\mathrm{T}}(\boldsymbol{w}_3 \times \boldsymbol{w}_2) = \boldsymbol{w}_2^{\mathrm{T}}(\boldsymbol{w}_1 \times \boldsymbol{w}_3) = \boldsymbol{w}_3^{\mathrm{T}}(\boldsymbol{w}_2 \times \boldsymbol{w}_1).$$

Examining Eq. (11) and Fig. 2 indicates that two types of angles can be defined to describe the force transmission behaviours of the robot at a specific configuration:

(1) The pressure angle φ_i within a limb

$$\varphi_i = \arccos(\boldsymbol{w}_i^{\mathrm{T}}(\boldsymbol{v}_i \times \boldsymbol{u}_i)), \quad i = 1, 2, 3. \tag{12}$$

This is the angle between the velocity (along $\boldsymbol{v}_i \times \boldsymbol{u}_i$) of point B_i, and the driving force (along $\boldsymbol{w}_i$) imposed by the proximal link to the distal link at the same point.

(2) The pressure angle γ_i amongst limbs

$$\gamma_1 = \arccos\left(\frac{\boldsymbol{w}_1^{\mathrm{T}}(\boldsymbol{w}_3 \times \boldsymbol{w}_2)}{|\boldsymbol{w}_3 \times \boldsymbol{w}_2|}\right),$$
$$\gamma_2 = \arccos\left(\frac{\boldsymbol{w}_2^{\mathrm{T}}(\boldsymbol{w}_1 \times \boldsymbol{w}_3)}{|\boldsymbol{w}_1 \times \boldsymbol{w}_3|}\right), \tag{13}$$
$$\gamma_3 = \arccos\left(\frac{\boldsymbol{w}_3^{\mathrm{T}}(\boldsymbol{w}_2 \times \boldsymbol{w}_1)}{|\boldsymbol{w}_2 \times \boldsymbol{w}_1|}\right).$$

In order to explain the physical meaning of γ_i, take γ_3 as an example. Assume that the proximal links 1 and 2 are locked. Then, the distal links 1 and 2 becomes a fictitious link. Thus, γ_3 represents the angle between the driving force (along $\boldsymbol{w}_3$) imposed by the distal link 3 to the fictitious link at point O', and the velocity (along $\boldsymbol{w}_2 \times \boldsymbol{w}_1$) of the same point.

Bearing in mind definition of the transmission angle,[18,19] we refer to $\varphi_i' = \pi/2 - \varphi_i$ as the transmission angle within a limb, and $\gamma_i' = \pi/2 - \gamma_i$ as the transmission angles amongst limbs. On the one hand, if $\varphi_i = \pi/2$ or $\varphi_i' = 0$, then $\boldsymbol{w}_i$, $\boldsymbol{u}_i$ and $\boldsymbol{v}_i$ are coplanar, leading to the singularity of the direct Jacobian, i.e. $\det(\boldsymbol{J}_q) \to 0$. In this case, the system loses at least 1-DOF. On the other hand, if $\gamma_i = \pi/2$ or $\gamma_i' = 0$, $\boldsymbol{w}_1, \boldsymbol{w}_2$ and $\boldsymbol{w}_3$ are coplanar, leading to the singularity of the indirect Jacobian, i.e. $\det(\boldsymbol{J}_x) \to 0$. This means that at least one uncontrollable degree of freedom is added to the system. In

https://doi.org/10.1017/S0263574711000622 Published online by Cambridge University Press

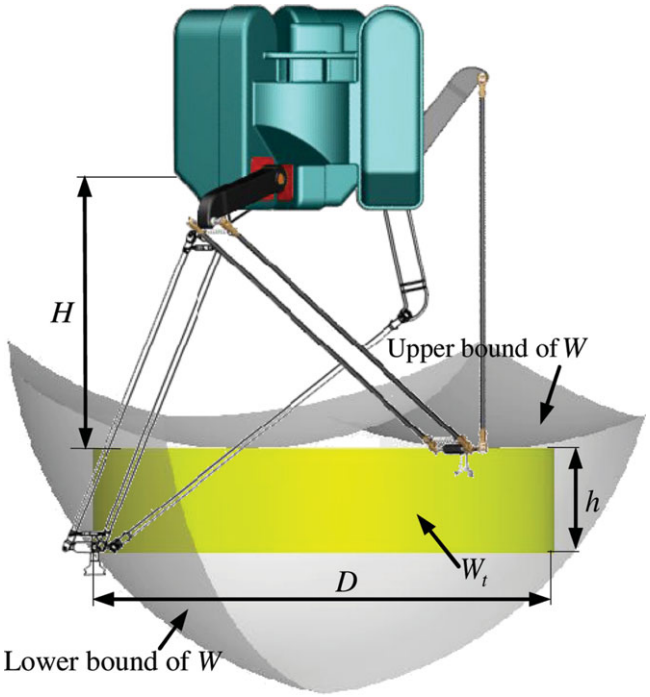

Fig. 3. (Colour online) The reachable and task workspaces.

addition, when $\varphi_i = \gamma_i = 0$ or $\varphi_i' = \gamma_i' = \pi/2$ $(i = 1, 2, 3)$, an isotropic configuration can be achieved. In summary, the pressure/transmission angles can be used to fully describe the direct and indirect singularities of the robot at a specific configuration.

4. Dimensional Synthesis

On the basis of foregoing analysis, dynamic dimensional synthesis will be conducted in what follows by using pressure/transmission angles to form the objective function and the constraints.

4.1. Workspace and design variables

As shown in Fig. 3, given l_1, l_2, e and H, the reachable workspace W of point O' is the intersection of the three subspaces associated with the three limbs because of the parallel architecture. Each subspace is the region enveloped by two spherical surfaces with l_2 being the radius. For pick-and-place operations, a cylindrical task workspace, denoted by W_t, of diameter D and modest height h can be tailored from W.

Given D, h ($\lambda_h = h/D = 0.2 \sim 0.25$) and cross sections of moving links, dynamic dimensional synthesis of the Delta robot can then be treated as a problem to determine the design variables l_1, l_2, e and H such that a good kinematic and dynamic performance can be achieved.

4.2. Dynamic performance index

It has been recognised that for high-speed pick-and-place operations, the driving torque $\boldsymbol{\tau}$ in Eq. (10) is primarily dominated by the inertial torque $\boldsymbol{\tau}_a$ in the acceleration and deceleration stages and by the centrifuge/Coriolis torque $\boldsymbol{\tau}_v$ when the robot is running at very high speed.

On the one hand, the inertial torque of a single actuated joint is given by

$$\tau_{ai} = I_A \boldsymbol{G}_i \ddot{\boldsymbol{r}}, \quad i = 1, 2, 3, \tag{14}$$

where $\boldsymbol{G}_i$ denotes the row of $\boldsymbol{G}$ associated with the ith limb, and

$$\begin{aligned}
\boldsymbol{G}_1 &= \frac{\eta l_1^2 \cos\varphi_1}{\cos\gamma_1} \frac{(\boldsymbol{w}_3 \times \boldsymbol{w}_2)^{\mathrm{T}}}{|\boldsymbol{w}_3 \times \boldsymbol{w}_2|} + \frac{\boldsymbol{w}_1^{\mathrm{T}}}{\cos\varphi_1}, \\
\boldsymbol{G}_2 &= \frac{\eta l_1^2 \cos\varphi_2}{\cos\gamma_2} \frac{(\boldsymbol{w}_1 \times \boldsymbol{w}_3)^{\mathrm{T}}}{|\boldsymbol{w}_1 \times \boldsymbol{w}_3|} + \frac{\boldsymbol{w}_2^{\mathrm{T}}}{\cos\varphi_2}, \\
\boldsymbol{G}_3 &= \frac{\eta l_1^2 \cos\varphi_3}{\cos\gamma_3} \frac{(\boldsymbol{w}_2 \times \boldsymbol{w}_1)^{\mathrm{T}}}{|\boldsymbol{w}_2 \times \boldsymbol{w}_1|} + \frac{\boldsymbol{w}_3^{\mathrm{T}}}{\cos\varphi_3}.
\end{aligned} \tag{15}$$

The maximum inertial torque of the ith actuated joint necessary to generate a unit acceleration of point O' at a specific configuration can be obtained by

$$\tau_{ai\,\max} = I_A \sqrt{\boldsymbol{G}_i \boldsymbol{G}_i^{\mathrm{T}}} = I_A \sqrt{\frac{\eta^2 l_1^2 \cos^2\varphi_i}{\cos^2\gamma_i} + \frac{1}{l_1 l_2 \cos^2\varphi_i} + 2\eta}. \tag{16}$$

It is easy to see from Eq. (17) that $\tau_{ai\,\max}$ can explicitly be expressed in terms of dimensional and inertial parameters as well as the pressure angles φ_i and γ_i. This means that occurrence of either direct or indirect singularity leads to $\tau_{ai\,\max} \to \infty$. Thus, the global maximum of $\tau_{ai\,\max}$ can be taken as a dynamic metric for minimisation, i.e.

$$\min_{\boldsymbol{x}} \left(\tau_{aG} = \max_{\boldsymbol{r} \in W_t} \{ \tau_{ai\,\max}(\boldsymbol{r}, \boldsymbol{x}) \} \right), \tag{17}$$

where $\boldsymbol{x} = (\, e \; l_1 \; l_2 \; H \,)$ denotes a set of design variables.

On the other hand, the centrifuge/Coriolis torque of a single actuated joint is given by

$$\tau_{vi} = I_A \dot{\boldsymbol{r}}^{\mathrm{T}} \boldsymbol{H}_i \dot{\boldsymbol{r}}, \tag{18}$$

where

$$\begin{aligned}
\boldsymbol{H}_i = \frac{1}{l_1^2 \Delta_i} \Bigg[& \frac{(\boldsymbol{v}_i \times \boldsymbol{u}_i)^{\mathrm{T}} (\boldsymbol{v}_i \times \boldsymbol{w}_i) \boldsymbol{w}_i \boldsymbol{w}_i^{\mathrm{T}}}{\Delta_i^2} \\
& + \frac{l_1}{l_2} \left(\boldsymbol{E}_3 - \frac{(\boldsymbol{v}_i \times \boldsymbol{u}_i) \boldsymbol{w}_i^{\mathrm{T}}}{\Delta_i} \right)^{\mathrm{T}} \left(\boldsymbol{E}_3 - \frac{(\boldsymbol{v}_i \times \boldsymbol{u}_i) \boldsymbol{w}_i^{\mathrm{T}}}{\Delta_i} \right) \Bigg].
\end{aligned}$$

Note that the Hessian matrix $\boldsymbol{H}_i$ only relates to $\boldsymbol{v}_i$, $\boldsymbol{u}_i$ and $\boldsymbol{w}_i$ within the ith limb. It can be seen that the direct singularity leads to $\tau_{vi} \to \infty$. Although τ_{vi} is nonlinear in terms of $\dot{\boldsymbol{r}}$, we may take the global maximum of the maximal singular value of $\boldsymbol{H}_i$

$$\tau_{vG} = \max_{\boldsymbol{r} \in W_t} \{ \sigma_{\max} (\boldsymbol{H}_i(\boldsymbol{r}, \boldsymbol{x})) \} \tag{19}$$

as an additional dynamic metric, which could serve as a check point of the validity of τ_{aG} by examining their consistency in terms of minimisation.

https://doi.org/10.1017/S0263574711000622 Published online by Cambridge University Press

Table I. Equivalent moments of inertia of the proximal link.

Descriptions	Value or expression
Moment of inertia I_{A1} contributed by the gearbox ($kg \cdot m^2$)	0.4714
Moment of inertia I_{A2} of the intermediate section ($kg \cdot m^2$)	$\mu_1 l_1^3/3$
Moment of inertia I_{A3} produced by the lump mass at B ($kg \cdot m^2$)	$m_b l_1^2$
Moment of inertia I_{A4} produced by the equivalent mass of distal links ($kg \cdot m^2$)	$4\mu_2 l_2 l_1^2/3$
Total moment of inertia I_A of the proximal link ($kg \cdot m^2$)	$I_{A1} + I_{A2} + I_{A3} + I_{A4}$

$m_b = 0.28$kg, $\mu_1 = 3.86$g/mm, $\mu_2 = 0.11$g/mm

4.3. Constraints

4.3.1. Dimensional constraints. The first dimensional constraint is the offset e that should be set such that

$$e \geq e_{\min}. \tag{20}$$

The reason for setting this constraint is that room should be made available for situating three servomotors on the base. Another constraint that should be taken into account is the workspace/machine volume ratio. For the pick-and-place robot, the constraint in this phase can be set by[2]

$$\delta = \frac{D}{2(e + l_1)} = 1.0 \sim 1.1. \tag{21}$$

Meanwhile, the following dimensional constraints should also be set to allow the mechanism to be assembled:

$$\sqrt{(H+h)^2 + (D/2+e)^2} - l_2 - l_1 < 0, \quad l_2 - l_1 - H < 0. \tag{22}$$

4.3.2. Transmission angle constraints. Velocity and accuracy are two important yet contradictory factors that should be considered in formulating performance constraints in the dimensional synthesis of the Delta robot. From $\dot{\boldsymbol{r}} = \boldsymbol{J}^{-1}\dot{\boldsymbol{q}}$, it can be seen that given $\|\dot{\boldsymbol{q}}\| = 1$, $\|\dot{\boldsymbol{r}}\|$ is minimised when the singular value of $\boldsymbol{J}^{-1}$ takes the minimum value, which is the reciprocal of the maximum singular value of $\boldsymbol{J}$. So, the maximum value of the maximal singular value of $\boldsymbol{J}$ throughout the entire task workspace should be minimised in order to achieve a higher velocity transmission ratio from the joint space to the Cartesian space, i.e.

$$\min_{\boldsymbol{x}} \max_{\boldsymbol{r} \in W_t} \sigma_{\max}(\boldsymbol{J}(\boldsymbol{r}, \boldsymbol{x})). \tag{23}$$

While, the minimum value of the minimal singular value of the Jacobian throughout the entire task workspace should be maximised in order to reduce the error transmission ratio from the joint space to the Cartesian space, i.e.

$$\max_{\boldsymbol{x}} \min_{\boldsymbol{r} \in W_t} \sigma_{\min}(\boldsymbol{J}(\boldsymbol{r}, \boldsymbol{x})). \tag{24}$$

Therefore, a trade-off can be made such that

$$\begin{cases} \min\limits_{\boldsymbol{r} \in W_t} \sigma_{\min}(\boldsymbol{J}(\boldsymbol{r}, \boldsymbol{x})) \geq b_l, \\ \max\limits_{\boldsymbol{r} \in W_t} \sigma_{\max}(\boldsymbol{J}(\boldsymbol{r}, \boldsymbol{x})) \geq b_u, \end{cases} \tag{25}$$

where b_u and b_l are the upper and lower bounds of the maximal and minimal singular values of the Jacobian in a global sense. However, the barrier encountered in practice is the difficulty to blindly choose proper b_u and b_l without a visible guidance. In order to overcome this problem, rewrite the inverse of the Jacobian

$$\begin{aligned} \boldsymbol{J}^{-1} &= \boldsymbol{J}_x^{-1}\boldsymbol{J}_q, \\ \boldsymbol{J}_x^{-1} &= \left[\frac{\boldsymbol{w}_3 \times \boldsymbol{w}_2}{|\boldsymbol{w}_3 \times \boldsymbol{w}_2|} \frac{1}{\cos\gamma_1} \quad \frac{\boldsymbol{w}_1 \times \boldsymbol{w}_3}{|\boldsymbol{w}_1 \times \boldsymbol{w}_3|} \frac{1}{\cos\gamma_2} \quad \frac{\boldsymbol{w}_2 \times \boldsymbol{w}_1}{|\boldsymbol{w}_2 \times \boldsymbol{w}_1|} \frac{1}{\cos\gamma_3} \right], \\ \boldsymbol{J}_q &= l_1 \mathrm{diag}[\cos\varphi_i]. \end{aligned} \tag{26}$$

It can be seen that given the actuators' movement error, the maximum value of γ_i throughout the entire workspace must be bounded by an allowable value $[\gamma]$ in order to restrain the error transmission ratio as $\gamma_i \to \pi/2$ leads to $\sigma_{\max}(\boldsymbol{J}^{-1}) \to \infty$. On the contrary, given the actuator rate, the maximum value of φ_i throughout the entire task workspace must be bounded by an allowable value $[\varphi]$ in order to ensure the velocity transmission ratio as $\varphi_i \to \pi/2$ leads to $\sigma_{\min}(\boldsymbol{J}^{-1}) \to 0$. Thus, the constraints in terms of the pressure/transmission angles can be formulated as follows:

$$\begin{aligned} &\max_{\boldsymbol{r} \in W_t} \gamma_{\max} \leq [\gamma], \gamma_{\max} = \max[\gamma_1\ \gamma_2\ \gamma_3], \\ &\max_{\boldsymbol{r} \in W_t} \varphi_{\max} \leq [\varphi], \varphi_{\max} = \max[\varphi_1\ \varphi_2\ \varphi_3]. \end{aligned} \tag{27}$$

Taking the advantage of visible expressions, the pressure /transmission angle constraints can be considered as an alternative of maximal/minimal singular value constraints given Eq. (26). The reasonable choice of $[\varphi]$ and $[\gamma]$ will be discussed in depth though an example in Section 5.

In what follows, the effects of the pressure/transmission angle constraint bounds on the feasible domains of the design variables will be discussed in detail via an example.

5. An Example

The proposed approach for dynamic dimensional synthesis will be carried out on the Delta robot with a cylindrical task workspace of $D = 1100$ mm in diameter and $h = 250$ mm in height. The moment of inertia of the proximal link and the equivalent mass of distal links are functions of link lengths and cross sections. The inertial parameters varying with the link lengths are listed in Tables I and II with μ_1 and μ_2 being the mass per unit length of the proximal and distal links, and m_b being a sum of the lumped mass of the proximal link at elbow B.

https://doi.org/10.1017/S0263574711000622 Published online by Cambridge University Press

Table II. Equivalent mass of the moving platform.

Descriptions	Value or expression
Mass of the moving platform itself m' (kg)	1.00
Equivalent mass m_e of the distal link at O' (kg)	$2\mu_2 l_2$
Total mass m (kg)	$m' + m_e$

$m_b = 0.28\,\text{kg}, \quad \mu_1 = 3.86\,\text{g/mm}, \quad \mu_2 = 0.11\,\text{g/mm}$

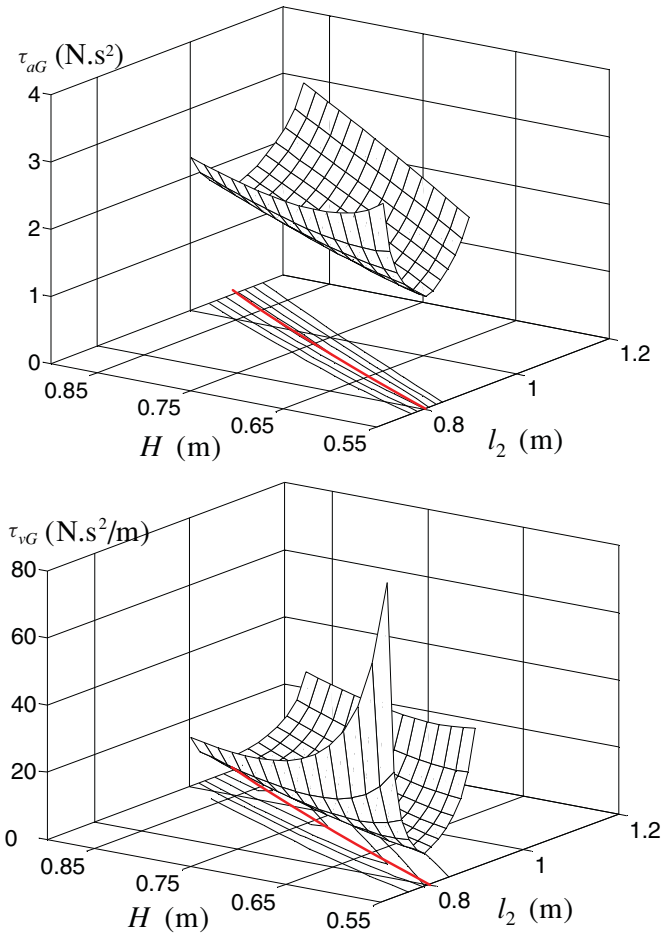

Fig. 4. (Colour online) Variations of τ_{aG} and τ_{vG} vs. H and l_2 given $l_1 = 0.35\,\text{m}$ and $e = 0.15\,\text{m}$.

Although the problem can be resolved by the sequential quadratic programming algorithm available in MATLAB Optimisation Tool Box, it would be helpful to have a deep insight into the effects of the pressure/transmission angle constraints on the feasible domains of design variables via a monotonic analysis.

Referring the ABB IRB 340 FlexPicker Delta robot, we take $\delta = 1.1$ and $e_{\min} = 0.15\,\text{m}$, leading to $l_1 = 0.35\,\text{m}$. Then, we investigate the effects of l_2 and H on τ_{aG} and τ_{vG} only considering the dimensional constraints given in Eq. (23). Observation of Fig. 4 shows that: (1) the distributions of τ_{aG} and τ_{vG} are extremely similar; (2) there is a continuous *curve* composed by the nearly linear relationship between H and l_2 such that τ_{aG} and τ_{vG} fall into the valleys of their distributions simultaneously; (3) along the valleys, τ_{aG} and τ_{vG} slightly decrease with the increase of H and l_2 along the

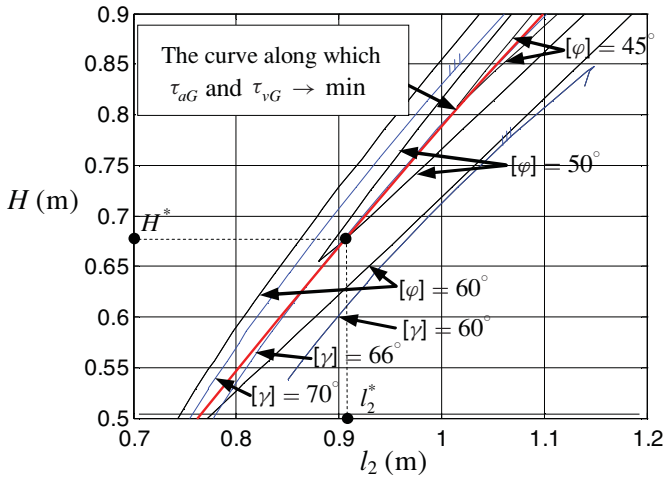

Fig. 5. (Colour online) Determination of the optimised H and l_2 given $l_1 = 0.35\,\text{m}$ and $e = 0.15\,\text{m}$.

curve. Thus, this validates the hypothesis of using τ_{aG} as the dynamic metric for minimisation.

Figure 5 shows the feasible domain of H and l_2 bounded by $[\varphi] = 40°, 50°, 60°$ and $[\gamma] = 60°, 70°$, respectively. It can be seen that the domain decreases with the decrease of $[\varphi]$, i.e. for achieving a large velocity transmission ratio, H and l_2 must take relatively larger values. Meanwhile, $[\gamma]$ must take relatively large value to ensure the *curve* is included in the feasible domain of H and l_2. Therefore, given a pair of $[\varphi]$ and $[\gamma]$, the optimised H^* and l_2^* can be obtained as the intersection of the contour bounded by $[\varphi]$ and the curve along which τ_{aG} falls into the valley of its distribution. It should be noted that the optimised $H^*$and l_2^* are also the minimum values. This is because increasing H and l_2 has little help for improving τ_{aG} but wastes materials and lowers the rigidity of the system. For example, given $[\varphi] = 50°$ and $[\gamma] = 70°$, we have $H^* = 0.675\text{m}$ and $l_2^* = 0.905\text{m}$. This leads to

$$\max_{\boldsymbol{r}\in W_t} \varphi_{\max} = [\varphi] = 50°, \quad \max_{\boldsymbol{r}\in W_t} \gamma_{\max} = 65.71° < [\gamma] = 70°,$$

$$\tau_{aG}^* = 1.231\text{N.s}^2, \quad \tau_{vG}^* = 2.153\,\text{N.s}^2/\text{m}.$$

In order to show the effectiveness of the proposed design approach, consider the existing ABB IRB 340 FlexPicker Delta robot with the dimensional parameters as follows:

$$e = 0.15\,\text{m}, \quad l_1 = 0.35\,\text{m}, \quad l_1 = 0.8\,\text{m}, \quad H = 0.58\text{m}.$$

For comparison purpose, assume that the inertial parameters of the robot are the same as those listed in Tables I and II. The computer simulation shows that

$$\max_{\boldsymbol{r}\in W_t} \varphi_{\max} = 58.02°, \quad \max_{\boldsymbol{r}\in W_t} \gamma_{\max} = 71.28°,$$

$$\tau_{aG} = 1.383\ \text{N} \cdot \text{s}^2, \quad \tau_{vG} = 4.779\ \text{N} \cdot \text{s}^2/\text{m}.$$

It is obvious that the proposed design could achieve a better kinematic and dynamic performance than the exiting design of the Delta robot.

https://doi.org/10.1017/S0263574711000622 Published online by Cambridge University Press

6. Conclusions

This paper presents an approach for dynamic dimensional synthesis of the Delta robot using the transmission angle constraints. The conclusions are drawn as follows:

(i) We define two types of transmission angles for the Delta robot, which enable the algebraic characteristics to be closely related to the geometry of the system, thereby can be used to describe the motion/force transmission behaviours in a visible manner.

(ii) We propose two dynamic metrics associated, respectively, with inertial and centrifuge/Coriolis components for minimisation. It has been shown that these metrics have a complete consistency. By setting a set of appropriate constraints in terms of the transmission angles, workspace/machine volume ratio, etc., we can obtain a set of optimised dimensional parameters for achieving good kinematic and dynamic performances throughout the entire workspace.

(iii) The proposed approach could be useful for the dynamic dimensional synthesis of other high-speed pick-and-place parallel robots driven by the proximal revolute joints, either the planar or the spatial.

Acknowledgments

The research is partially supported by the National High Technology Research and Development Program of China (Grant No.2007AA04Z245), the National Natural Science Foundation of China (Grant No. 50775158, 50675151) and the Ph.D. Programs Foundation of Ministry of Education (Grant No. 20060056018).

References

1. T. Huang, M. Li, Z. X. Li, D. G. Chetwynd and D. J. Whitehouse "Planar parallel *robot* mechanism with two translational degrees of freedom," *US Patent*, 7090458 B2 (2006).
2. T. Huang, Z. X. Li, M. Li, D. G. Chetwynd and C. M. Gosselin "Conceptual design and dimensional synthesis of a novel 2-DOF translational parallel robot for pick-and-place operations," *ASME J. Mech. Des.* **126**, 449–455 (2004).
3. R. Clavel, "Device for the movement and positioning of an element in space," *US Patent*, 4976582 (1990).
4. R. Clavel, "A Fast Robot with Parallel Geometry," *Proceedings of the 18th International Symposium on Industrial Robots*, Lausanne, Switzerland (1988) pp. 91–100.
5. F. Pierrot and O. Company, "H4: A New Family of 4-dof Parallel Robots," *Proceedings of IEEE/ASME International Conference on Advanced Intelligent Mechatronics*, Atlanta, USA (1999) pp. 508–513.
6. V. Nabat, M. Rodriguez, O. Company, S. krut and F. Pierrot "Par4: Very High Speed Parallel Robot for Pick-And-Place," *Proceedings of the IEEE International Conference on Intelligent Robotic Systems* (*IROS*), Edmonton, Alberta (2005) pp. 553–558.
7. T. Yoshikawa, "Manipulability of robotic mechanisms," *Int. J. Robot. Res.* **4**(2), 439–446 (1985).
8. K. Zanganeh and J. Angeles, "Kinematic isotropy and the optimum design of parallel manipulators," *Int. J. Robot. Res.* **6**, 185–197 (1997).
9. D. Chablat, P. Wenger and J. Angeles, "The Iso-Conditioning Loci of a Class of Closed-Chain Manipulators," *Proceedings of IEEE International Conference on Robotics and Automation (ICRA),* Leuven, Belgium (1998) pp. 1970–1975.
10. C. M. Gosselin and J. Angeles, "The optimum kinematic design of a spherical 3-DOF parallel manipulator," *J. Mech. Transm. Autom. Des.* **111**(2), 202–207 (1989).
11. T. Huang, D. J. Whitehouse and J. S. Wang, "Local dexterity, optimum architecture and design criteria of parallel machine tools," *CIRP Ann.* **47**(1), 347–351 (1998).
12. C. M. Gosselin and J. Angeles, "A globe performance index for the kinematic optimization of robotic manipulators," *ASME J. Mech. Des.* **113**, 220–226 (1991).
13. K. Miller, "Maximization of workspace volume of 3-DOF spatial parallel manipulator," *ASME J. Mech. Des.* **124**, 347–350 (2002).
14. K. Miller, "Optimal design and modeling of spatial parallel manipulators," *Int. J. Robot. Res.* **23**(2), 127–140 (2004).
15. M. A. Laribi, L. Romdhane and S. Zeghloul, "Analysis and dimensional synthesis of the Delta robot for a prescribed workspace," *Mech. Mach. Theory* **42**, 859–870 (2007).
16. H. Choi, A. Konno and M. Uchiyama, "Design, implementation, and performance evaluation of a 4-dof parallel robot," *Robotica* **28**(1), 107–118 (2010).
17. T. Huang, M. Li, Z. X. Li, D. G. Chetwynd and D. J. Whitehouse "Optimal kinematic design of 2-DOF parallel manipulators with well-shaped workspace bounded by a specified conditioning index," *IEEE Trans. Robot. Autom.* **20**(3), 538–542 (2004).
18. J. W. H. Sun and K. J. Waldron, "Graphical transmission angle control in planar linkage synthesis," *Mech. Mach. Theory* **14**, 385–397 (1981).
19. S. S. Balli and S. Chand, "Transmission angle in mechanisms," *Mech. Mach. Theory* **37**, 175–195 (2002).
20. X. J. Liu, C. Wu and J. S. Wang, "A New Index for the Performance Evaluation of Parallel Manipulators: A Study on Planar Parallel Manipulators," *Proceeding of the 6th World Congress on Intelligent Control and Automation (WCICA),* Chongqing, China (2008) pp. 353–357.
21. O. Ma and J. Angeles, "Optimum Design of Manipulators Under Dynamic Isotropy Conditions," *Proceedings of the IEEE International Conference on Robotics and Automation (ICRA),* Atlanta, USA (1993) pp. 470–475.
22. T. Yoshikawa, "Dynamic manipulability of robot manipulators," *J. Rob. Syst.* **2**(1), 113–124 (1985).
23. S. Tadokoro, I. Kimura and T. Takamori, "A Measure for Evaluation of Dynamic Dexterity Based on a Stochastic Interpretation of Manipulator Motion," *Proceedings of the IEEE International Conference on Robotics and Automation (ICRA)*, Pisa, Italy (1991) pp. 509–514.
24. A. Codourey, "Dynamic modelling of parallel robots for computed-torque control implementation," *Int. J. Robot. Res.* **17**(12), 1325–1336 (1998).
25. K. Miller, "Experimental Verification of Modeling of Delta Robot Dynamics by Direct Application of Hamilton's Principle," *Proceedings of the IEEE International Conference on Robotics and Automation (ICRA),* Nagoya, Japan (1995) pp. 532–537.
26. H. Choi, A. Konno and M. Uchiyama, "Inverse Dynamic Analysis of a 4-DOF Parallel Robot H4," *Proceedings of the IEEE International Conference on Intelligent Robotic Systems (IROS),* Sendai, Japan (2004) pp. 3501– 3506.
27. T. Huang, J. P. Mei, Z. X. Li and X. M. Zhao "A method for estimating servomotor parameters of a parallel robot for rapid pick-and-place operations," *ASME J. Mech. Des.* **127**, 596–601 (2005).

https://doi.org/10.1017/S0263574711000622 Published online by Cambridge University Press